ГЛАСНИК Српског географског друштва 106(1) 567-580
BULLETIN OF THE SERBIAN GEOGRAPHICAL SOCIETY 2026

Original scientific paper UDC 551.4:556(65)
https://doi.org/10.2298/GSGD2601567S

Received: February 6, 2026
Corrected: March 26, 2026
Accepted: May 11, 2026

Saddek Samai[1]*, Leila Benhenni*, Leila Bouchama**

**Geophysics laboratory, University of Sciences and Technology Houari Boumadiene, Algiers, Algeria*

***Laboratoire villes Région et Gouvernance, University of Sciences and Technology Houari Boumadiene, Algiers, Algeria*

INTEGRATED GEOPHYSICAL AND LITHOLOGICAL ANALYSIS OF A SEMI-ARID KARST BASIN FOR SUSTAINABLE WATER MANAGEMENT: WADI ZOUZFANA (SOUTH-WESTERN ALGERIA)

Abstract: Semi-arid regions are often characterized by strong spatial heterogeneity of geological formations, surface processes, and groundwater circulation, which critically control water availability and land use planning. This study investigates the subsurface structure of the Wadi Zouzfana basin (south-western Algeria) using an integrated approach combining vertical electrical sounding (VES) and lithological data from three core boreholes (21–30 m depth). Twenty-four VES measurements were conducted using the Schlumberger configuration (AB = 200 m) and calibrated against borehole logs to establish reliable resistivity–lithology relationships in a karstified carbonate environment. Five main geoelectrical units were identified, corresponding to recent alluvium, karstified limestone, transitional carbonates, weathered dolomite, and compact bedrock. Low resistivity values (100–600 Ω·m) dominate the wadi axis, reflecting water-saturated alluvial deposits and karstified limestone, while higher resistivities (>1200 Ω·m) characterize structurally uplifted carbonate formations along the basin margins. Spatial interpolation of resistivity data within a GIS framework reveals an asymmetric bedrock morphology controlled by NE–SW tectonic structures, with a central depression guiding surface runoff concentration and groundwater storage. The results highlight the strong geomorphological and structural control on groundwater distribution and infiltration potential in this semi-arid karst basin. The integrated geophysical–lithological methodology provides a cost-effective framework for site-scale subsurface characterization applicable to similar semi-arid karst environments and supports sustainable water resource management and land planning in data-scarce arid environments.

Keywords: vertical electrical sounding, lithological calibration, karst basin characterization, hydrogeography, groundwater distribution, GIS spatial analysis, semi-arid Algeria

[1] ssamai@usthb.dz (corresponding author)
Leila Benhenni (https://orcid.org/0009-0001-3691-159X)
Leila Bouchama (https://orcid.org/0009-0009-9668-645X)

Introduction

Water scarcity in semi-arid regions affects over 2 billion people globally (UN-Water, 2021), with North Africa particularly vulnerable due to irregular rainfall, high evaporation rates (>2000 mm/year), and climate change impacts (IPCC, 2021). Understanding subsurface structure and hydrogeological functioning is essential for controlling runoff, enhancing groundwater recharge, and ensuring water security. However, spatial characterization of water resources depends critically on subsurface knowledge—particularly in karst terrains where dissolution processes create heterogeneous permeability and complex groundwater circulation patterns.

Vertical Electrical Sounding (VES) provides cost-effective subsurface characterization (Telford et al., 1990; Reynolds, 2011), proven effective across North Africa for aquifer assessment (Ben Salem et al., 2023; Ouerghi et al., 2018; El Yaouti et al., 2017). Recent advances combining electrical resistivity with GIS spatial analysis enhance basin-scale hydro geographical applications (Samouëlian et al., 2005; Kirsch, 2009; Kebede et al., 2023, Tiaiba et al., 2025). However, most studies focus on groundwater exploration rather than integrated basin characterization (Metwaly and AlFouzan, 2013; Charboui et al., 2024), and few systematically integrate borehole calibration with regional VES surveys to establish robust resistivity-lithology relationships in karst environments.

This study addresses this gap by calibrating VES measurements with three core boreholes in Wadi Zouzfana basin, southwestern Algeria, to provide a reproducible framework for local-scale hydrogeographical characterization. The objectives are to: (1) establish calibrated resistivity-lithology relationships for karst carbonates; (2) map subsurface structure within the investigated sector to characterize local groundwater distribution and water retention capacity; and (3) provide geospatial data supporting water conservation and land productivity in data-scarce semi-arid environments.

Beyond engineering applications, subsurface characterization in semi-arid karst environments provides essential insight into basin-scale hydrological functioning, groundwater recharge mechanisms, and spatial water availability.

Study Area and Geological Setting

Geographic and Climatic Context

The investigation site is located in Wadi Zouzfana basin, Beni-Ounif municipality, Bechar Province, southwestern Algeriamm, 110 km east of Bechar city. The investigated sector corresponds to a localized area of approximately 1.26 hectares within the broader Wadi Zouzfana, selected for detailed hydrogeological characterization (Figure 1). The region experiences extreme aridity with annual precipitation (Figure 2), ranging 1.2-31.5 mm (1999-2018 period) and mean temperatures of 25.89°C, creating severe water stress for approximately 13,000 inhabitants (density 1.01 persons/km^2). Temperature analysis shows interannual mean of 25.89°C, with maximum recorded in 2018 (27.37°C) and minimum in 2000 (24.07°C). These extreme climatic conditions, emblematic of Saharan climate, necessitate stringent water resource management.

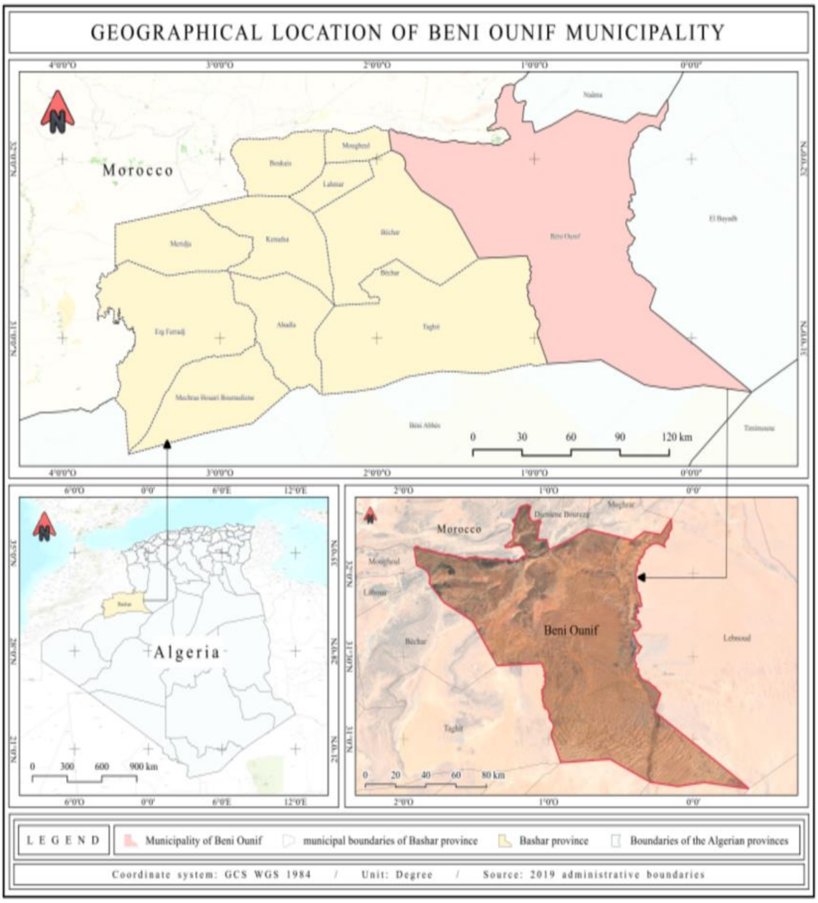

Fig. 1. Geographical context of the study area

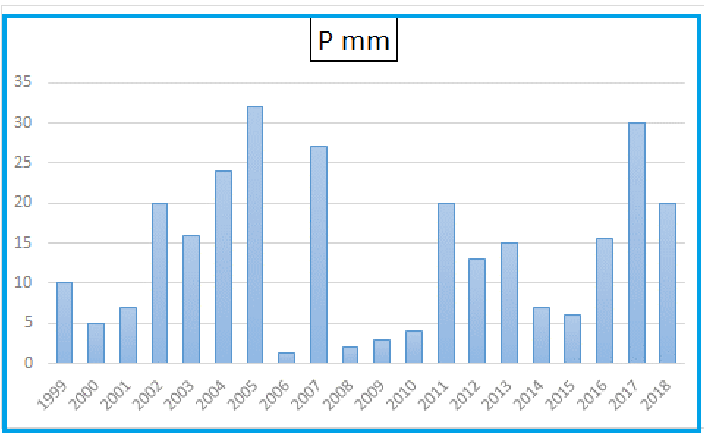

Fig. 2. Histogram illustrating mean annual precipitation variations from 1999 to 2018

Hydrogeological Context

The Wadi Zouzfana originates in the Ksour Mountains at approximately 1600 m elevation, covering about 16,600 km² with a total length of 360 km before meeting Wadi Guir in the Igli area. Geological assessments indicate that the watercourse serves as a critical source of sand derived from erosion of dominant sandstone formations, particularly in upstream regions near Djebel Maiz, as well as from colluvial and alluvial deposits (Laborde, 2003). The investigated sector corresponds to a local reach within the Wadi Zouzfana basin where detailed subsurface characterization is required for water management infrastructure planning.

The Ksour Mountains constitute a section of the Saharan Atlas, a complex intracratonic mountain range affected by tectonic processes (Mekahli, 1998; Douihasni, 1976), extending over 1000 km and characterized by Jurassic-generation coffered folds (Flamand, 1911). The stratigraphic sequence demonstrates predominance of middle and upper Jurassic epochs, characterized by deltaic complexes, alongside lower to upper Cretaceous timeframes encompassing fluvial and marl deposits. Jurassic anticline formations are interspersed with extensive synclinal structures where Cretaceous sandstones are exposed (Bassoulet, 1973; Delfaud, 1973; Kazi-Tani, 1986; Chaouche et al., 2001). These formations are associated with inverse fault systems and profound overlaps affecting topography and sand transportation patterns (Salhi, 2002).

The area is characterized by Cretaceous carbonate formations—predominantly dolomitic limestone with varying degrees of weathering, fracturing, and karstification. NE-SW oriented tectonic structures control wadi morphology and karst development (Mekahli, 1998; Chaouche et al., 2001). The ephemeral hydrological regime generates high-intensity flood events that transport sediments and create alluvial deposits in the wadi bed. Karst dissolution processes create secondary porosity with heterogeneous permeability, presenting specific challenges for water retention including potential losses through clay-filled cavities.

Geomorphological Context

The geomorphological setting is extensively influenced by fluvial erosion within a highly contorted tectonic framework. Sedimentary deposits, including limestone, marl, and sandstone, subjected to faulting and folding along NE-SW orientation, have culminated in topographical configuration characterized by asymmetric cuestas and valleys (Salhi, 2002; Fortas, 2017). The wadi channel is located within these tectonic depressions, conforming to geological axes of weakness. Fluvial erosion processes in such semi-arid basin environments are known to generate significant chemical and mechanical sediment loads (Manojlović et al., 2012), contributing to the alluvial deposits observed in the wadi bed.

Basin slopes are intersected by ravines and secondary talwegs, while the valley floor is covered with modern deposits. Sand and gravel deposits, mainly derived from sandstone erosion, undergo local modifications influenced by seasonal water movements. The present morphological characteristics include generally low slopes, lateral colluvium accumulations, and a sparsely populated alluvial plain. These landform features are crucial for assessing site stability, water infiltration capacity, and basin water storage potential.

Materials and Methods

VES Methodology

Twenty-four VES measurements were conducted along three east-west profiles (P1, P2, P3) spaced 30 m apart, with 8 soundings per profile at 30 m intervals. The Schlumberger configuration was used with electrode spacing up to AB=200 m, providing investigation depths of approximately 50 m. The apparent resistivity ρ_a is expressed by:

$$\boldsymbol{\rho_a = K.\frac{\Delta V}{I}} \tag{1}$$

Where K denote the geometric factor associated with the measurement array. In context of the Schlumberger configuration, this factor can be expressed as:

$$K = \frac{\left(\frac{AB}{2}\right)^2 - \left(\frac{MN}{2}\right)^2}{MN} \tag{2}$$

Each measurement comprised 14 acquisition levels with progressively increasing electrode spacings (Keller & Frischknecht, 1966). Although borehole data constrain lithological interpretation to depths of 21–30 m, VES inversion with AB/2 up to 100 m provides resistivity models extending to approximately 50–70 m depth. Borehole calibration was applied to the upper layers, and resistivity-lithology relationships were extrapolated to deeper layers based on consistent geoelectrical contrasts identified in the inversion models.

Borehole Drilling and Calibration

Three core boreholes (B1, B2, B3) were strategically drilled to depths ranging from 21 to 30 meters to provide lithological ground-truth data (Figure 3). Borehole locations were selected to represent principal geological settings: B1 on the right bank (weathered dolomitic zones), B2 in the wadi axis (alluvial deposits), and B3 on the left bank (karstified limestone outcrops). Continuous core sampling enabled detailed lithological logging at 1-meter intervals (Figure 4), documenting rock type, weathering degree, fracture intensity, and karst features including dissolution cavities and clay infilling.

VES measurements were conducted at these borehole locations to enable direct calibration. VES data were inverted using IPI2Win software (Bobachev, 2002) with iterative least-squares optimization. The calibration process involved systematic correlation of geoelectrical layer boundaries with lithological contacts, establishing resistivity ranges for each formation type. Inversion quality was assessed using root mean square (RMS) error:

$$RMS = \sqrt{\frac{\sum(\rho_a^{measured} - \rho_a^{calculated})^2}{n}} \times 100\% \tag{3}$$

where $\rho_a^{measured}$ and $\rho_a^{calculated}$ represent measured and calculated apparent resistivities, respectively, and n is the number of measurement points.

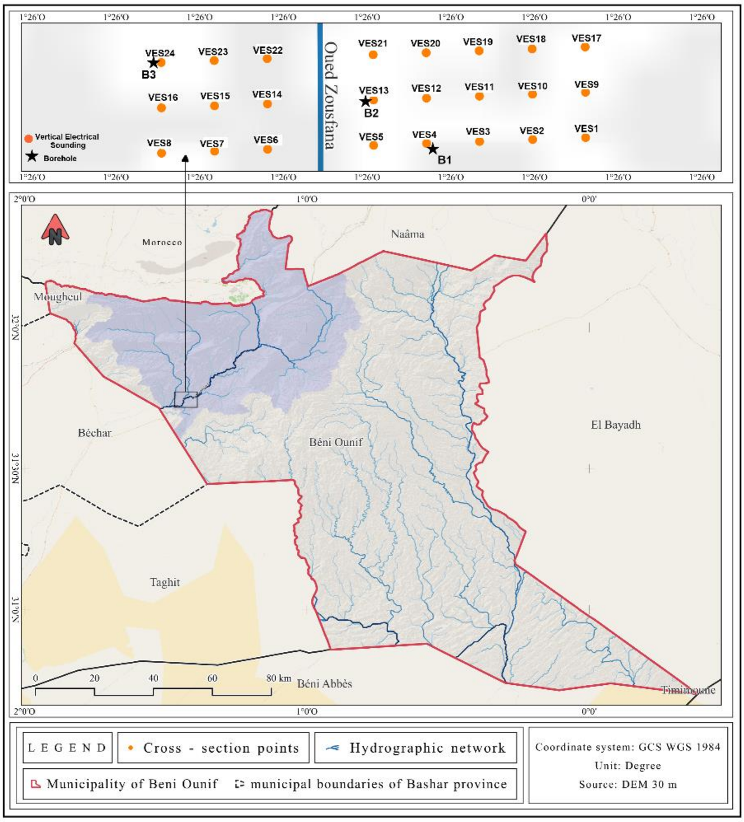

Fig. 3. Location map of VES stations and core boreholes

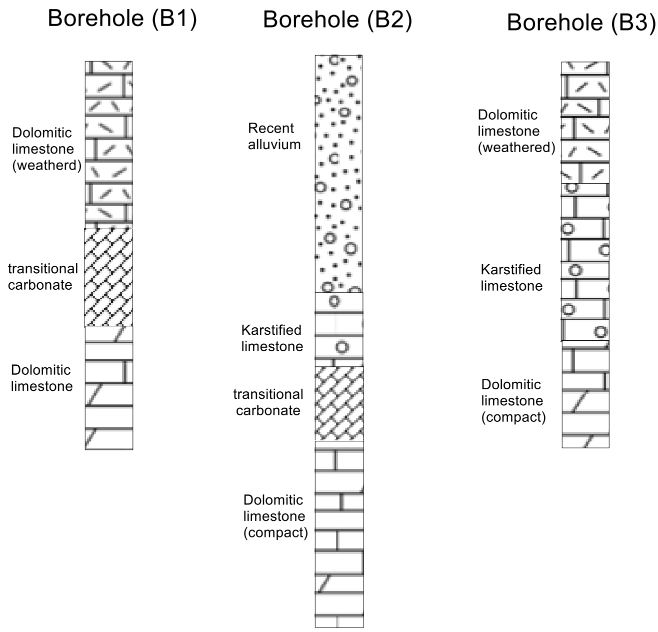

Fig. 4. Lithological logs of boreholes B1, B2, and B3

GIS Integration

All VES and borehole locations were georeferenced (UTM Zone 31N, WGS84). Resistivity data were interpolated using kriging to generate maps at investigation depths corresponding to AB=40 m (~8-10 m depth) and AB=100 m (~25-30 m depth). Bedrock depths from calibrated VES inversions were interpolated to create continuous bedrock topography surfaces for basin morphology analysis and water storage capacity estimation.

Results

Resistivity Calibration and Geoelectrical Unit Identification

Electrical resistivity values from VES inversions were calibrated using lithological data from three core boreholes drilled to depths of 21-30 meters. All VES inversions at borehole locations achieved excellent quality with RMS errors below 1.4% (B1: 0.825%, B3: 1.32%, B2: 0.733%), validating the reliability of the resistivity models. Five main geoelectrical units were identified (Table 1).

Table 1. Calibrated Resistivity Ranges and Lithological Interpretation

Geological Formations	***Resistivity [Ω·m]***	***Validation Boreholes***	***Interpretation***
Recent alluvium	100-200	B2	Holocene sandy-gravel deposits saturated with groundwater
Karstified limestone	300-600	B2, B3	Cretaceous limestone with secondary porosity, clay-filled karst cavities
Transitional carbonate	700-1000	B1, B2	Fractured dolomitic and sandy-calcareous limestone, moderate permeability
Weathered dolomite	900–1200	B1, B3	Shallower wheathered zone partially unsaturated vadose zone
Compact dolomite	1200–1600	B1, B2, B3	Compacted bedrock

The calibrated resistivity ranges are consistent with published values for carbonate formations in semi-arid regions. Karstified limestone (300-600 Ω·m) falls within ranges reported by Chalikakis et al. (2011) for karst systems (100-900 Ω·m) and Bensaoula and Adjim (2017) for western Algerian karst aquifers (120-850 Ω·m). Transitional carbonates (700-1000 Ω·m) and compact dolomite (900-1200 Ω·m) are consistent with typical dolomitic formations (500-5000 Ω·m); (Telford et al., 1990; Palacky, 1987).

The progressive deepening of competent bedrock from B1 (21 m) through B3 (24 m) to B2 (30 m) reflects buried karst valley morphology oriented along the wadi axis. These established resistivity ranges provide a robust framework for interpreting the additional 21 VES measurements across the study area.

Geographic Resistivity Mapping and Bedrock Topography

Spatial analysis of geoelectrical data enabled generation of continuous resistivity surfaces at two investigation depths and comprehensive bedrock topography mapping.

Resistivity at AB=40 m (~8-10 m Depth)

Resistivity mapping at AB=40 m reveals three distinct domains (Figure 5). The western sector, including the wadi bed, exhibits low to moderate resistivities (200-600 Ω·m), with particularly low values (<400 Ω·m) corresponding to recent alluvium (100-200 Ω·m) and karstified limestone (300-600 Ω·m). The central zone shows intermediate resistivities (600-1200 Ω·m), suggesting transitional carbonates (700-1000 Ω·m) and weathered dolomite (1200-1600 Ω·m). The eastern sector displays very high values (>4000 Ω·m), indicating consolidated dolomitic limestone at or near surface with exceptional desaturation.

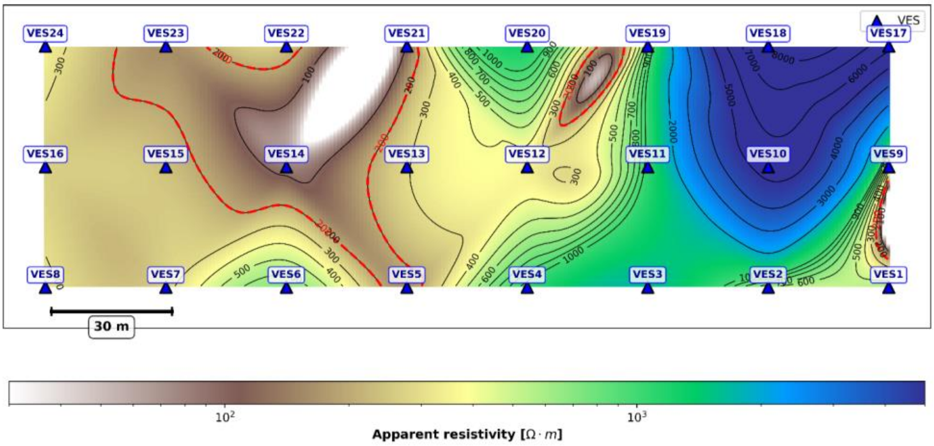

Fig. 5. Resistivity map at AB=40 m

Resistivity at AB=100 m (~25-30 m Depth)

At AB=100 m depth, lateral zonation persists with attenuated contrasts (Figure 6). The western domain maintains low resistivity (200-400 Ω·m), consistent with karstified limestone beneath alluvial cover. The bank zone displays intermediate values (400-900 Ω·m) representing transitional carbonates approaching compact bedrock. The eastern resistive anomaly persists with maximum values of 1500-2600 Ω·m, confirming vertical continuity of consolidated formations to at least 30 m depth.

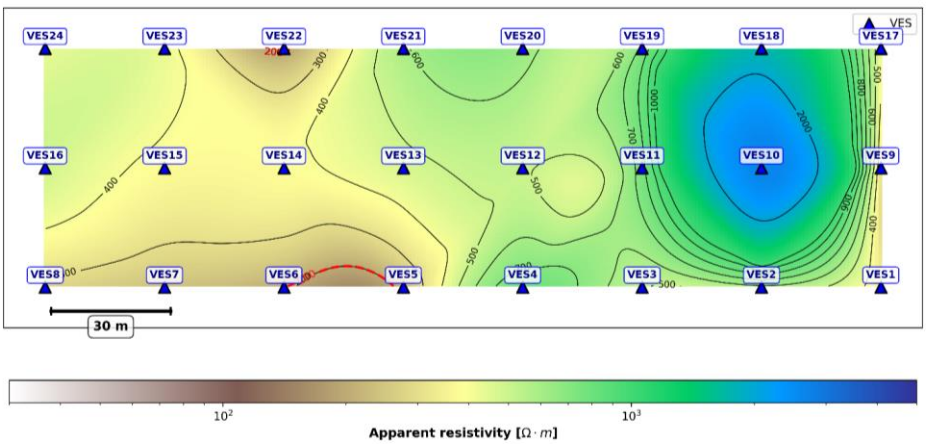

Fig. 6. Resistivity map at AB=100 m

Bedrock Topography

Bedrock topography mapping reveals asymmetric structure controlling wadi geometry (Figure 7). Both banks display bedrock uplifts with depths ranging 60-70 m, corresponding to structural flanks where compact dolomitic limestone is encountered at relatively shallow depths. In contrast, the wadi bed shows shallowest bedrock depths (<58 m), indicating central depression aligned with the wadi course. This configuration reflects buried karst valley morphology oriented along the NE-SW tectonic trend, consistent with regional structural patterns.

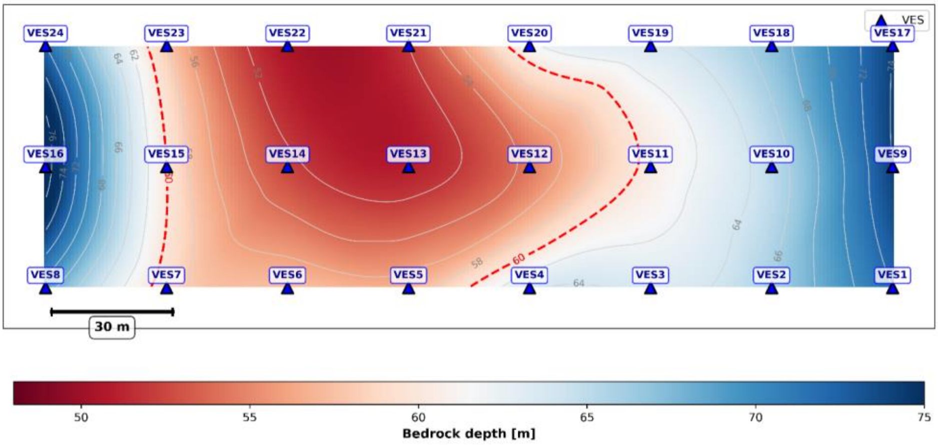

Fig. 7. Bedrock topography map

Vertical Geoelectrical Profiles

Three east-west oriented geoelectrical profiles (P1, P2, P3), each composed of eight VES measurements, were established to investigate vertical resistivity structure (Figure 8). The inverted resistivity data were visualized as pseudo-sections with topographic correction.

Profile P1 reveals resistive zones (1000-2000 Ω·m) predominating in deeper parts below 70-80 m elevation, interpreted as compact dolomitic bedrock. The upper portion shows low resistivity (<200 Ω·m), indicating recent alluvium. Intermediate zones (300-700 Ω·m) correspond to karstified limestone and transitional carbonates.

Profile P2 shows high contrast between central conductive zone and lateral resistive zones. The wadi bed exhibits low resistivity (<200 Ω·m), while both banks display high values (>1000 Ω·m). A localized conductive anomaly (300-600 Ω·m) at approximately 160-170 m distance suggests enhanced karstification requiring consideration in water management planning.

Profile P3 demonstrates progressive lateral variation from west to east, with low resistivity in the wadi bed (<300 Ω·m), intermediate values on the left bank (300-1000 Ω·m), and very high resistivity on the right bank (>1000 Ω·m), indicating asymmetric subsurface structure.

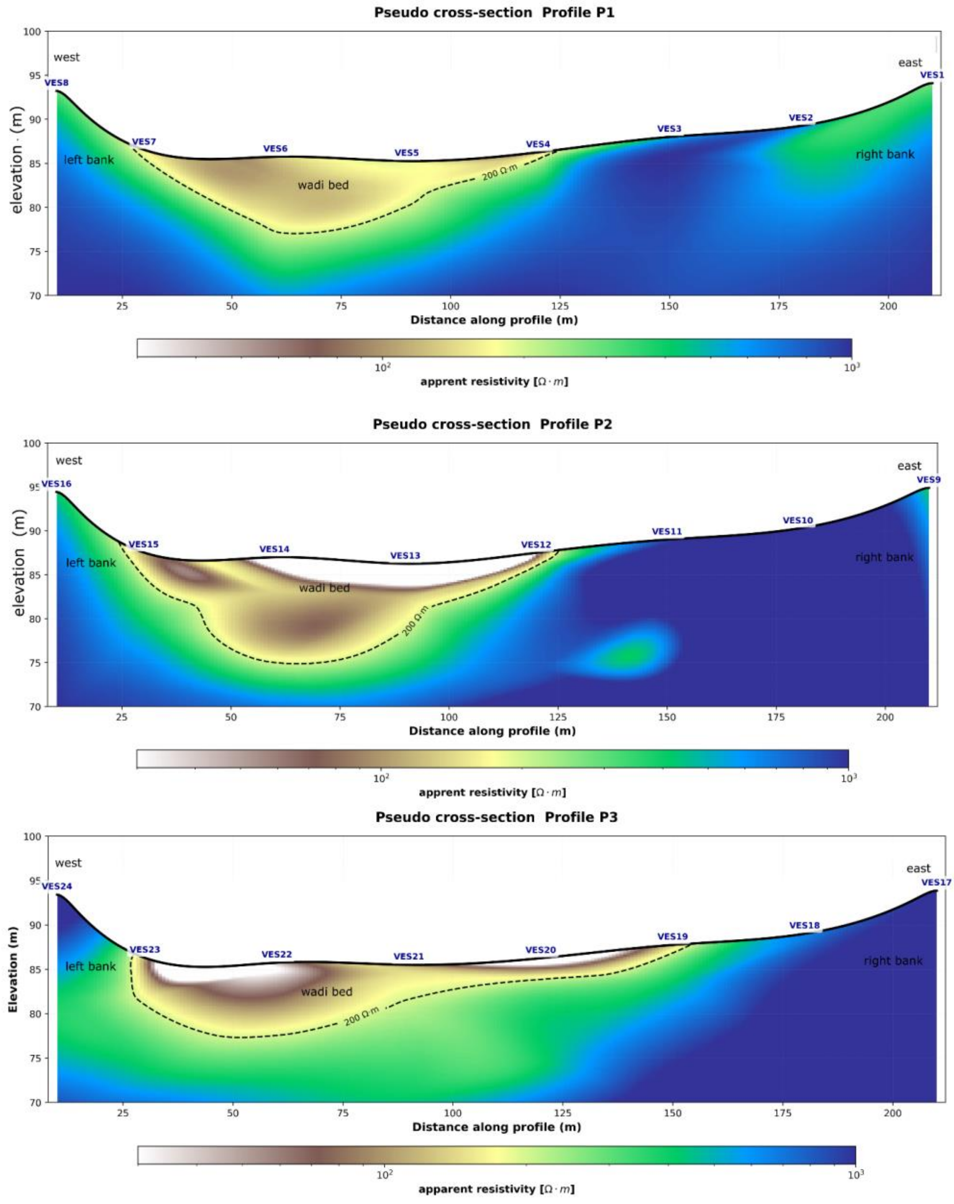

Fig. 8. Pseudo sections corresponding to the three selected profiles

Discussion

Tectono-Geomorphological Control on Subsurface Architecture

The bedrock topography reveals characteristic asymmetric morphology controlled by NE-SW tectonic structures inherited from the Saharan Atlas. Structural uplifts on both banks (depths 60-70 m) contrast with central depression beneath the wadi bed (depths <58 m), defining distinct geomorphological domains that directly control spatial distribution of alluvial deposits, karst development, and groundwater flow patterns. This asymmetric configuration reflects the interplay between tectonic inheritance and fluvial-karst processes in shaping the present-day basin geometry. It should be noted that bedrock depths exceeding 30 m are constrained by VES inversion alone, without direct borehole verification. These estimates carry greater uncertainty and should be interpreted with caution pending further drilling confirmation.

The karstified limestone unit (300-600 Ω·m) represents a critical hydrogeological feature with heterogeneous permeability. Significant thickness variation from 8 m at B2 to 20 m at B3 reflects structural control on karst development, with more extensive dissolution occurring in uplifted structural positions. The consistent resistivity value of 400 Ω·m, despite thickness variations, indicates mature karst systems with clay-filled cavities and high water content, characteristic of semi-arid karst evolution where limited recharge reduces active dissolution.

The localized conductive anomaly in Profile P2 (300-600 Ω·m at 160-170 m distance) suggests enhanced karstification or preferential groundwater accumulation within the carbonate sequence. Such features represent zones of enhanced secondary permeability that strongly influence groundwater circulation and water retention within the basin, requiring careful consideration in basin-scale water management strategies.

Spatial Organization of Hydrogeological Units and Water Distribution

The integrated geoelectrical characterization reveals the spatial organization of hydrogeological units controlling water distribution and retention capacity. The compact dolomitic bedrock (1200- 1600 Ω·m), consistently identified at 21-30 m depths, represents low-permeability substrate with minimal fracturing that underlies the entire basin. Structural uplifts on both banks (60-70 m depth) define the lateral boundaries of the basin, controlling surface runoff concentration and subsurface water accumulation in the central depression.

Karstified limestone zones (300-600 Ω·m, thickness 8-20 m) represent areas of enhanced secondary permeability that strongly influence groundwater circulation and water retention within the basin. The distribution and thickness of these zones, mapped through calibrated resistivity analysis, indicates that enhanced permeability is greatest in the wadi bed and left bank areas where karstified formations are thickest. Understanding the spatial distribution of these permeable zones enables targeted water management strategies that optimize retention while accounting for potential water losses through interconnected karst networks.

The interconnected system of surficial water-saturated alluvium (100-200 Ω·m) and underlying karstified limestone aquifer constitutes the primary natural water storage mechanism in the basin. By understanding spatial distribution of these permeable zones through calibrated resistivity mapping, basin-scale water management can incorporate strategies that enhance infiltration during flood events while accounting for natural losses through karst circulation, maximizing water availability for agricultural and domestic uses in the semi-arid environment.

The asymmetric bedrock topography, with central depression morphology validated through borehole-VES correlation, defines the basin water storage geometry. The mapped bedrock surface enables accurate estimation of basin storage capacity (approximately 285,000 m^3) essential for flood management planning and water resource allocation. This storage capacity supports water security for approximately 13,000 inhabitants and agricultural development across 1,200 hectares of potentially irrigable land. These hydrogeographical constraints strongly influence settlement patterns, agricultural practices, and long-term land use sustainability in the Wadi Zouzfana basin.

Methodological Advances for Local-Scale Subsurface Characterization

This study demonstrates effectiveness of integrating limited but strategically placed borehole data with regional VES surveys to establish robust resistivity-lithology relationships in complex karst terrains. The calibration approach, achieving excellent VES inversion quality (RMS <1.4%) and consistent resistivity ranges across multiple boreholes, provides a replicable methodology for local-scale hydrogeographical characterization with potential applicability at broader scales when combined with additional data in data-scarce semi-arid regions.

The established resistivity ranges enable interpretation of 21 additional VES measurements without requiring further drilling, reducing investigation costs by an estimated 75% compared to conventional drilling-only approaches. These calibrated ranges (recent alluvium: 100-200 Ω·m; karstified limestone: 300-600 Ω·m; transitional carbonates: 700-1000 Ω·m; weathered dolomite: 900–1200 Ω·m; compact bedrock: 1200–1600 Ω·m) provide reference values applicable to similar Cretaceous carbonate formations throughout the Saharan Atlas and broader North African region, contributing to regional hydrogeographical understanding.

Despite robust basin-scale characterization, the one-dimensional VES inversion assumes horizontally layered earth structures, which may oversimplify lateral heterogeneity in complex karst terrains. The localized conductive anomaly in Profile P2 suggests three-dimensional features requiring additional investigation through electrical resistivity tomography or other 2D/3D imaging methods to fully characterize spatial variability of karst permeability at the basin scale.

Conclusion

This integrated study successfully characterized subsurface geology of Wadi Zouzfana basin through 24 vertical electrical soundings calibrated with three core boreholes (21-30 m depth). The calibration process achieved excellent inversion quality (RMS errors <1.4%), establishing five geoelectrical units with well-defined resistivity ranges applicable throughout the Saharan Atlas region.

Regional resistivity mapping revealed clear structural asymmetry reflecting tectono-geomorphological control on basin geometry. The central wadi sector exhibits low resistivities (200-600 Ω·m) indicating water-saturated alluvial deposits overlying karstified limestone, while the eastern sector displays high resistivities (>1500 Ω·m) indicating consolidated dolomitic limestone at shallow depth. Bedrock topography mapping reveals structural uplifts on both banks (60-70 m depth) defining basin boundaries, contrasting with central depression (<58 m) controlling surface runoff concentration and groundwater storage geometry (285,000 m^3 capacity).

The satisfactory agreement between calibrated VES results and borehole lithology supports the reliability of the methodology for subsurface characterization in semi-arid karst environments, though further independent verification would strengthen these findings. Mapped karstified limestone zones (thickness 8-20 m) represent areas of enhanced secondary permeability strongly influencing groundwater circulation and water retention patterns. A localized conductive anomaly in Profile P2 (300-600 Ω·m at ~160 m distance) indicates enhanced karstification requiring consideration in basin-scale water management.

This borehole-calibrated geophysical methodology reduces investigation costs by approximately 75% compared to conventional drilling-only approaches while maintaining high reliability. The approach provides essential decision-support for basin-scale water and land development in Saharan regions, enabling evidence-based planning of water management infrastructures that enhance both water security and land productivity for 13,000 inhabitants and 1,200 hectares of irrigable land in climatically stressed environments, directly supporting Sustainable Development Goal 6.

Conflict of Interest: The authors declare no conflict of interest.

References

Bassoulet, J.P. (1973). Étude stratigraphique du Mésozoïque de l'Atlas saharien occidental (Algérie). Notes et Mémoires du Service Géologique de l'Algérie, 15, 1-184.

Ben Salem, S., Chkir, N., & Zouari, K. (2023). Integrated geophysical and hydrochemical approach for groundwater potential assessment in arid Tunisia. *Journal of African Earth Sciences,* 198, Article 104795.

Bensaoula, F., & Adjim, M. (2017). Contribution of geophysical methods in the study of karst aquifers: Case of Tafna catchment, northwestern Algeria. *Arabian Journal of Geosciences,* 10(8), 174.

Bobachev, A.A. (2002). IPI2Win: A Windows software for an automatic interpretation of resistivity sounding data. Moscow State University.

Chalikakis, K., Plagnes, V., Guerin, R., Valois, R., & Bosch, F.P. (2011). Contribution of geophysical methods to karst-system exploration: An overview. *Hydrogeology Journal*, 19(6), 1169-1180. DOI:10.1007/s10040-011-0746-x

Chaouche, A.K., Aït Ouali, R., Bracene, R., Derder, M.E., & Djellit, H. (2001). Chronologie de l'ouverture du bassin des Ksour (Atlas Saharien, Algérie) au début du Mésozoïque. *Bulletin de la Société Géologique de France*, 172(3), 285-293. https://doi.org/10.2113/172.3.285

Charboui, S., Maanan, M., & El Ouardi, H. (2024). Application of electrical resistivity tomography for groundwater exploration in semi-arid regions: A review. *Environmental Earth Sciences,* 83(2), 45.

Delfaud, J. (1973). Le Jurassique de l'Atlas Saharien occidental. Bulletin de la Société Géologique de France, 15(3-4), 167-168.

Douihasni, M. (1976). Étude géologique de la région d'Aïn Ouerka-Boussemghoune (partie centrale des Monts des Ksour). Analyse structurale [Doctoral dissertation, Université d'Oran].

El Yaouti, F., El Mandour, A., Khattach, D., Benavente, J., & Kaufmann, O. (2017). Salinization processes in the unconfined aquifer of Bou-Areg (NE Morocco): A geostatistical, geochemical, and tomographic study. *Applied Geochemistry,* 85, 85-98. DOI 10.1016/j.apgeochem.2008.10.005

Flamand, G.B.M. (1911). Recherches géologiques et géographiques sur le Haut-Pays de l'Oranie et sur le Sahara. Lyon, France.

Fortas, S. (2017). Géomorphologie et risques naturels dans les Monts des Ksour [Doctoral dissertation, Université d'Oran 2].

IPCC. (2021). Climate Change 2021: The Physical Science Basis. Contribution of Working Group I to the Sixth Assessment Report. Cambridge University Press.

Kebede, A., Takele, T., & Tsegaye, A. (2023). Integrated geophysical and GIS-based approach for groundwater potential zone mapping in the crystalline terrain of central Ethiopia. *Geomechanics and Geophysics for Geo-Energy and Geo-Resources*, 9(1), 23.

Keller, G.V., & Frischknecht, F.C. (1966). Electrical Methods in Geophysical Prospecting. Pergamon Press.

Kirsch, R. (2009). Groundwater Geophysics: A Tool for Hydrogeology (2nd ed.). Springer.

Laborde, J.P. (2003). Éléments d'hydrologie de surface. Agence Nationale des Ressources Hydrauliques, Alger.

Manojlović, P., Mustafić, S., & Mladenović, B. (2012). Chemical and mechanical water erosion ratio in the Mlava River basin. *Bulletin of the Serbian geographical society*, 92(1), 27-46. https://doi.org/10.2298/GSGD1201027M

Mekahli, L. (1998). Évolution des Monts des Ksour (Algérie) de l'Héttangien au Bajocien: biostratigraphie, sédimentologie, paléogéographie et stratigraphie séquentielle. Documents du Laboratoire de Géologie de Lyon, 144, 227.

Metwaly, M., & AlFouzan, F. (2013). Application of 2-D geoelectrical resistivity tomography for subsurface cavity detection in the eastern part of Saudi Arabia. *Geoscience Frontiers*, 4(4), 469-476. https://doi.org/10.1016/j.gsf.2012.12.005

Ouerghi, S., Kouzana, L., Majdoub, R., & Ben Mammou, A. (2018). Groundwater prospecting using the electrical resistivity method: A case study from southeastern Tunisia. *Arabian Journal of Geosciences*, 11(20), 641.

Palacky, G.J. (1987). Resistivity characteristics of geologic targets. In M.N. Nabighian (Ed.), Electromagnetic Methods in Applied Geophysics (Vol. 1, pp. 53-129). Society of Exploration Geophysicists. https://doi.org/10.1190/1.9781560802631.ch3

Reynolds, J.M. (2011). An Introduction to Applied and Environmental Geophysics (2nd ed.). Wiley-Blackwell.

Salhi, A. (2002). Les phénomènes d'ensablement des infrastructures dans les Monts des Ksour: cas de la zone Djenien Bourezg - Béni Ounif [Master's thesis, Université d'Oran 2].

Samouëlian, A., Cousin, I., Tabbagh, A., Bruand, A., & Richard, G. (2005). Electrical resistivity survey in soil science: A review. *Soil and Tillage Research*, 83(2), 173-193. 10.1016/j.still.2004.10.004

Telford, W.M., Geldart, L.P., & Sheriff, R.E. (1990). Applied Geophysics (2nd ed.). Cambridge University Press.

Tiaiba, M., Merzouk, B., Bensefia, S., & Herizi, T. (2025). Groundwater quality assessment using spatio-temporal evolution of water quality index and GIS in K'sob watershed (semiarid area-east Algeria). *Bulletin of the Serbian geographical society,* 105(2), 157-174. DOI:10.2298/GSGD2502157T

UN-Water. (2021). Summary Progress Update 2021: SDG 6 – Water and Sanitation for All. United Nations.